Mem. S.A.It. Vol. 77, 282

Memorie della

Direct imaging photometry with the MOST satellite⋆

J.F. Rowe[1], J.M. Matthews[1], R. Kuschnig[1], D.B. Guenther[2], A.F.J. Moffat[3], S.M.R. Rucinski[4], D. Sasselov[5], G.A.H. Walker[1], W.W. Weiss[6]

[1]Department of Physics and Astronomy, University of British Columbia 6224 Agricultural Road, Vancouver BC V6T 1Z1, Canada e-mail: rowe@astro.ubc.ca
[2]Department of Astronomy and Physics, St. Mary's University Halifax, NS B3H 3C3, Canada
[3]Département de physique, Université de Montréal C.P. 6128, Succ. Centre-Ville, Montréal, QC H3C 3J7, Canada
[4]David Dunlap Observatory, University of Toronto P.O. Box 360, Richmond Hill, ON L4C 4Y6, Canada
[5]Harvard-Smithsonian Center for Astrophysics 60 Garden Street, Cambridge, MA 02138, USA
[6]Institut für Astronomie, Universität Wien Türkenschanzstrasse 17, A–1180 Wien, Austria

Abstract. Canada's first space telescope, MOST (Microvariablity and Oscillations of Stars) was successfully launched on June 30, 2003 with a primary mission to perform ultra-high-precision photometry to detect acoustic oscillations in solar-like stars. MOST has the ability to observe single fields for uninterrupted periods of up to two months and targets can be observed either through Fabry lens imaging or Direct imaging. This report reviews the Direct imaging capabilities of the MOST satellite and the extraction of accurate stellar photometry.

Key words. MOST ; ultra-precise photometry

1. Introduction

The MOST satellite orbits in a 820-km-high circular Sun-synchronous polar orbit with a period of 101.413 minutes. The satellite utilizes a 15-cm optical telescope with a CCD photometer behind a single broadband filter (350 - 750 nm) and is capable of monitoring stars nearly continuously for up to 8 weeks in a Continuous View Zone with a declination range of $+36^\circ \geq \delta \geq -18^\circ$. The satellite was initially designed to achieve photometric precision of a few parts per million (ppm ∼ μmag) at frequencies greater than 1 mHz in the Fourier domain. To achieve the necessary photometric stability an array of Fabry microlenses projects an extended image of the instrument pupil on to the Science CCD (a 1K × 1K E2V 47-20 detector). For stars brighter than V ∼ 6.5 this Fabry Imaging mode can reach the desired precision for observing runs of at least one month.

Although not part of the original science design, fainter stars can be monitored (V ≥

Send offprint requests to: J.F. Rowe

7) (simultaneously, or independently of the Fabry Imaging mode) in an open area of the Science CCD not covered by the 6×6 Fabry microlens array and its chromium field stop mask. In the Direct Imaging field, defocused star images are projected, with a Full-Width Half-Maximum (FWHM) of about 2.5 pixels. (The focal plane scale of MOST is about 3 arcsec/pixel.) The photometric precision possible in the Direct Imaging Mode is not as good as for the Fabry photometry as Direct Imaging targets are fainter and more sensitive to CCD calibrations. However, the unprecedented duty cycle of the MOST observations and the thermal/mechanical stability of the instrument yield impressive results. The point-to-point precision of the photometry for a 7.5 magnitude star is about 3 millimag for a 1.5s exposure during low stray light conditions, with sampling rates as high as 10 exposures per minute. For example, for MOST's first Primary Science Target, Procyon, the $V = 8$ star HD 61199 was chosen for the Direct Imaging field and was discovered to be a multiperiodic δ Scuti pulsator (see Fig. 2c in Matthews et al. (2004)) with a peak amplitude of about 1 millimag.

The MOST instrument was designed to obtain fixed extended pupil images of a single bright target star through a Fabry microlens. In this way, the Fabry Imaging measurements are insensitive to pointing wander of the satellite. The Direct Images, however, do reflect the pointing errors. In data from the satellite commissioning and its early scientific operations, pointing errors of up to about 10 arcsec led to wander of the Direct Images of up to 3 pixels on the CCD. This made precision photometry vulnerable to uncalibrated sensitivity variations among adjacent pixels. The pointing performance of MOST has been dramatically improved since thanks to upgraded software and a better understanding of the mechanical performance of the reaction wheels in its attitude control system. The pointing performance of the satellite has been improved dramatically since its early operation, now consistently giving positional errors of about ± 1 arcsec ~ 0.3 pixel *rms*. This stability has resulted in improved photometry especially beneficial for Direct Imaging giving a stable PSF for modeling and flat fielding errors have become less relevant.

2. MOST Direct Imaging Photometry

MOST is a microsatellite (mass = 54 kg; peak solar power = 39 W) with limited onboard processing capability, memory, and downlink. Hence it is not possible to transfer the entire set of 1024×1024 pixels of the Science CCD to Earth at a rapid sampling rate and with an ADC (Analogue-to-Digital Conversion) of 14 bits. Small segments of the CCD ("subrasters") are stored, which contain key portions of the target field. This usually includes the Primary Science Target Fabry Image, 7 adjacent Sky Background Fabry Images, and subrasters for dark and bias readings and several nearby Secondary Science Targets in the Direct Imaging field (less than about 0.5° away). Typical dimensions for Direct Imaging targets is 20×20 pixels. Examples of MOST raw data and a document describing the FITS file and header format in detail are available in the MOST Public Data Archive at the MOST Mission website: www.astro.ubc.ca/MOST.

2.1. Photometric Reduction

In general, the approach to reducing MOST Direct Imaging photometry is similar to groundbased CCD photometry, applying traditional aperture and PSF (Point-Spread Function) approaches to the subrasters. However, there are several aspects and challenges specific to MOST data. For example, the MOST instrument has no on-board calibration lamp for correction of pixel-to-pixel sensitivity variations ("flatfielding"). There are also phases of increased stray light from scattered Earthshine which repeat regularly during each satellite orbit (P = 101 min). We will describe the basics of the data reduction process here, but a more detailed description of the Direct Imaging data reduction can be found in Rowe et al. (2005).

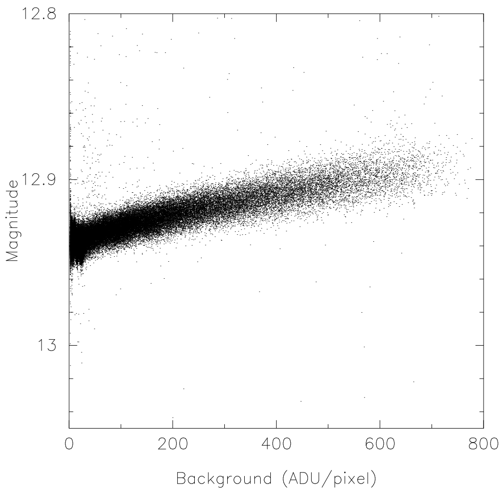

Fig. 1. The relationship between the instrumental magnitude and the background level as measured on the CCD frame.

2.2. Instrumental Corrections

To lower cost and increase reliability, the MOST instrument has no moving parts, so there is no mechanical shutter which can cut off light to the entire CCD for dark measurements; exposures are ended by rapid charge transfer into a frame buffer on the CCD. Dark measurements are obtained from portions of the CCD shielded from light by a chromium mask above the focal plane. Despite the lack of an on-board calibration lamp, it is possible to recover some flatfielding information for each subraster by exploiting intervals of high stray light during certain orbital phases. Frames containing no detectable stars are chosen from the data set. Such frames can be obtained when the satellite is commanded to point to an "empty" field (with only stars much fainter than V = 13), or occasionally, when the satellite loses fine pointing and the stars wander outside their respective subrasters. During two weeks of observing, over which 50,000 - 100,000 individual exposures are typically obtained, about 2000 - 4000 flatfielding frames are usually available from when the satellite loses fine pointing. The stray light can produce a strong spatial gradient across the CCD, so a 2-dimensional polynomial is fitted to all the available flatfielding pixels and removed. For each subraster, the mean pixel value is measured and compared to each individual pixel value; a linear fit to the correlation is made. The slope of this relationship is the relative gain and the zero point is the dark current. The relative pixel gains are found to vary by less than 2% across any individual subraster, with the standard deviation for any individual pixel less than 0.5%.

2.3. PSF Fitting and Adding Up the Starlight

After determination of the star positions and the background, the PSF for each star is fitted by either a Moffat profile (Moffat 1969) or a Gaussian function. In general it is found that the Moffat profile provides a better approximation of the PSF shape. The PSF is computed independently for each subraster using the Levenberg-Marqardt approach (Press et al. 1992) to find the best fit parameters. Once the stellar source has been modeled, the total flux is estimated by using aperture photometry for the centre of the model fit and using the model fit for the faint extended wings. For targets obtained early in the mission lifetime before substantial pointing improvements, such as ξ Gemini, this step is important as the aperture accounts for the smearing effects of pointing jitter not included in the model and the model allows an estimation of stellar flux located outside the subraster. The FWHM of the PSF under good tracking is found to be about 2 pixels, but the stellar source can be easily traced out to a radius of 8 pixels, meaning for large pointing deviations a significant portion of flux can lie outside the subraster. With more recent targets where the pointing accuracy is greatly improved, only the PSF model is necessary to determine the brightness of the source. The final magnitude is defined as

$$mag = 25.0 - 2.5 * \log\left(\frac{F_p + F_r}{E_t} g\right), \qquad (1)$$

as the standard conversion between magnitude and flux, where F_p is the flux in ADU measured from the PSF fit, F_a is the flux residual inside a small aperture in ADU, E_t is the

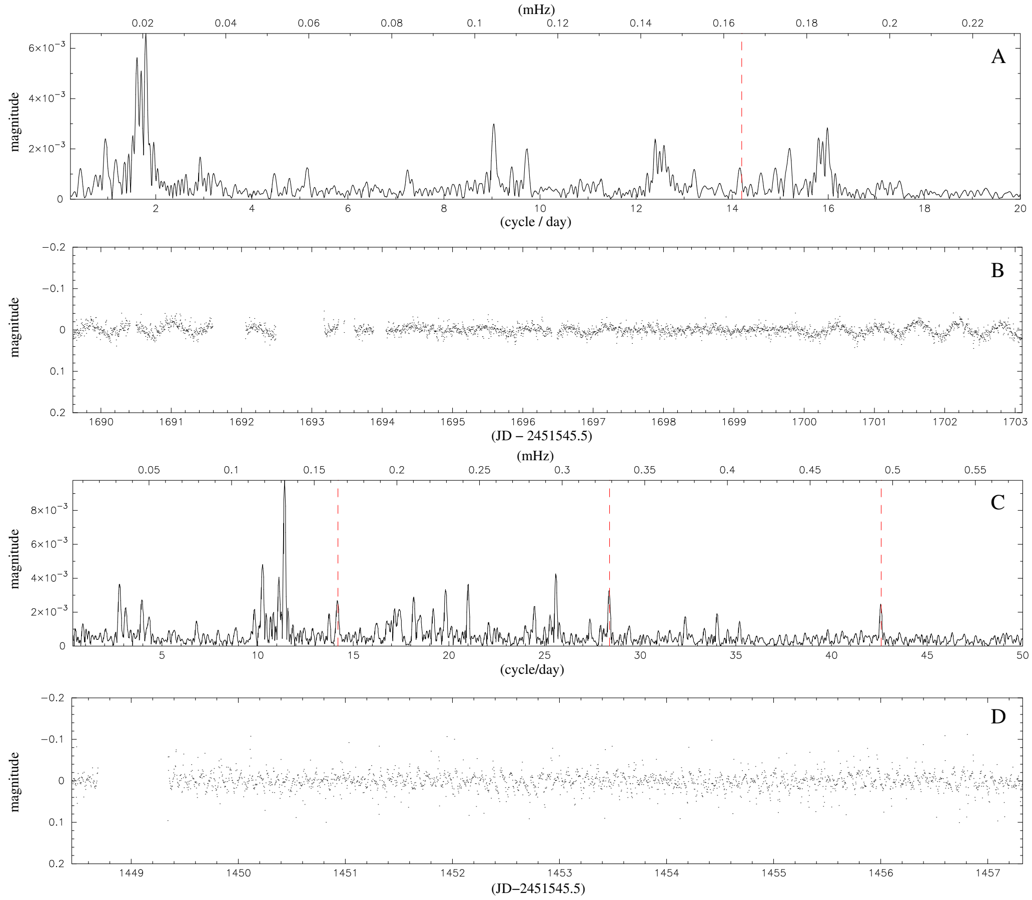

Fig. 2. Fourier amplitude spectra and lightcurves for the stars BD+18 4914 and HD 263551. Panel A shows the Fourier amplitude spectrum and Panel B shows the light curve from observations of the γ Doradus type variable star BD+18 4914 (V=10.6). Panel C shows the Fourier amplitude spectrum and Panel D shows the light curve for the δ Scuti type variable star HD 263551 (V=9.7). The light curves have been binned by 5 minute intervals. The dashed vertical lines in the amplitude spectrum mark the orbital frequency and harmonics of the satellite.

exposure time in seconds and g is the gain in e^{-}/ADU. The zero point of 25 has been arbitrarily chosen.

2.4. Removal of Stray Light Effects

It was discovered that the background level needs to be scaled to properly remove the contribution from stray light. The cause of this effect may be related to the 2D fits to remove gradients from the subrasters are not sufficient. With the small number of subraster pixels higher order polynomial fits are not stable, hence the estimation of the background level is not optimum. Regardless, it can be corrected for. In Figure 1,

the relationship between instrumental magnitude and the background level is shown. A fit is made between the stellar flux and the background level either with a polynomial or a cubic spline depending on the complexity of the relationship. If the relationship is modeled with a cubic spline, then the original data are binned before the fit, with 500 data points per bin and a minimum bin width of 10 ADU (Analogue-to-Digital Units) per pixel. In most cases the peak-to-peak amplitude of stray light variations is reduced by this approach to a few $\times$ 0.1 millimag. It can be further reduced by techniques such as subtracting a running, averaged background phased to the orbital period (Rucinski et al. 2004). The advantage of the simple approach taken here is that no prior knowledge of the orbital period is required and the amplitude of the stray light component is allowed to vary from orbit to orbit with changes in the Earth's albedo.

3. Results

We present light curves from observing runs of HD 209458 and ξ Gemini. Fabry observations of ξ Gemini where acquired from 20 - 28 of December 2003. Panel A of Figure 2 shows the Fourier amplitude spectrum of the star BD+18 4914 (V=10.6) observed in conjuncture with the transiting planetary system HD 209458. Panel B shows the light curve where data points have been binned by 5 minute intervals. Observations of 14 days spanned from 14 - 30 August 2004. This star has a spectral class of F5 and shows γ Doradus type pulsations with strong frequencies detected at 1.5 - 2.0 cycles per day. There are also high δ Scuti like frequencies seen at 9-10 cycles per day. The amplitude of the strongest frequency is at 6 mmag and the noise level is better than 0.05 mmag and the duty cycle for the observations is 85%.

The star HD 263551 (V=9.7) was chosen for simultaneous Direct Imaging observations because of its spectral class (A7). Panel C of Figure 2 shows the Fourier amplitude spectrum. Observations were acquired from 20 - 28 December 2003. The noise level is better than 0.1 mmag and amplitude of the largest signal (or discovery amplitude) is less than 1 mmag. There are more than 12 frequencies easily identifiable. The light curve is shown in Panel D. The data points have been binned by 5 minute intervals. These observations where obtained during the commissioning phase of the satellite and the pointing performance was not ideal with an average wander of 6" during the observations. We are still able to extract useful photometry.

For each observing run the MOST satellite has the capability of simultaneously monitoring multiple stars. This was not part of the original design plans, but thanks to much better than expected pointing performance, the Direct Imaging mode has provided a very useful mode for observations. While the photometric point-to-point performance may not be as good in Fabry modes, the high duty cycle and rapid data acquisition rate are being to yield some impressive results.

References

Matthews, J.M. et al. 2004, Nature, 430, 51
Moffat, A.F.J. 1969, A&A, 3, 455
Press, W.H. Teukolsky, S.A. Vetterling, W.T. Flannery, B.P. 1992, Numerical Recipes in Fortran 77 Second Edition, Cambridge University Press, 678
Rowe, J.F. et al. 2005, ApJ, submitted
Rucinski, S.M. et al. 2004, PASP, 116, 1093